resources

MDPI

Article

Integrated Assessment of Potentially Toxic Elements in Soils and Irrigation Water and Human Health Risk in a Gold Mining-Impacted Area of Southern Ecuador

Juan González-Menéndez [1], Carlos Hugo Bustamante-Torres [1], Bryan Salgado-Almeida [2], Giannella Muriel-Granda [3], Samantha Jiménez-Oyola [1,4] and Kenny Escobar-Segovia [1,*]

1 Faculty of Engineering in Earth Sciences, Escuela Superior Politécnica del Litoral (ESPOL) Polytechnic University, Campus Gustavo Galindo, Km. 30.5 Vía Perimetral, Guayaquil 090902, Ecuador; juajgonz@espol.edu.ec (J.G.-M.); chbustam@espol.edu.ec (C.H.B.-T.); sjimenez@espol.edu.ec (S.J.-O.)
2 Instituto Geológico y Minero de España (IGME-CSIC), C/Matemático Pedrayes 25, 33005 Oviedo, Spain; bj.salgado@igme.es
3 Facultad de Postgrado, Universidad Espíritu Santo (UEES), Samborondón 092301, Ecuador; giannellamuriel@uees.edu.ec
4 EC-Water, Academic and Research Network, Geo-Engineering and Advanced Processes Research Laboratory (GEA-RLab), Escuela Superior Politécnica del Litoral (ESPOL) Polytechnic University, Campus Gustavo Galindo, Km. 30.5 Vía Perimetral, Guayaquil 090902, Ecuador
* Correspondence: kescobar@espol.edu.ec

Abstract

Areas where mining activities overlap with agricultural production may promote the mobilization of potentially toxic elements (PTEs) into soils and water resources, thereby creating exposure pathways for populations living or working in these environments. This study analyzes the concentration of PTEs in agricultural soils and irrigation water from Santa Rosa, southern Ecuador, and assesses the associated health risks for exposed agricultural workers. For this purpose, 35 soil samples were collected from farms and 12 water samples from the irrigation canal during the dry season of 2025. The concentration of PTEs in soil and water was determined using X-ray fluorescence (XRF) and inductively coupled plasma mass spectrometry (ICP-MS), respectively. The PTE concentration in both matrices was compared with the maximum permissible limits (MPL) established by Ecuadorian regulations. Non-carcinogenic hazard indices (HI) and carcinogenic risk (TCR) were estimated following the U.S. EPA methodology. In soil, As and Cr were the PTEs of greatest concern, exceeding the MPL in 93% of the samples and by up to 4.4 and 2.4 times, respectively, while in water, all PTEs were below the MPL. Non-carcinogenic risk was below the recommended limit for soil and water ($HI_{soil} = 3.00 \times 10^{-2}$ and $HI_{water} = 2.00 \times 10^{-3}$), with As as the dominant contributor. Cancer risk was tolerable in soil ($TCR_{soil} = 4.34 \times 10^{-5}$), while in water it remained at a low level ($TCR_{water} = 1.65 \times 10^{-6}$). These findings identify As and Cr as priority contaminants and support targeted monitoring and source-control measures in mining-influenced agricultural areas. Overall, by integrating agricultural soil and irrigation water quality with an occupational health risk assessment in Santa Rosa, this study contributes evidence to support future research in mining–agriculture coexistence areas.

Keywords: heavy metals; environmental contamination; non-carcinogenic risk; carcinogenic risk; risk assessment

Check for updates

Academic Editor: Brad Ridoutt

Received: 15 May 2026
Revised: 12 June 2026
Accepted: 17 June 2026
Published: 22 June 2026

Copyright: © 2026 by the authors. Licensee MDPI, Basel, Switzerland. This article is an open access article distributed under the terms and conditions of the Creative Commons Attribution (CC BY) license.

1. Introduction

Agricultural areas influenced by metallic mining represent complex environmental settings where the mobilization of potentially toxic elements (PTEs) from mineralized zones and mining wastes can degrade soil and water quality. This process facilitates the transfer of contaminants into agricultural systems, increasing potential exposure pathways for populations living and working in these environments [1–3].

At a global scale, the accumulation of PTEs in agricultural soils has been widely reported in regions where mining districts overlap with productive land use. Studies conducted in countries such as China, South Africa, and several regions of Latin America have documented elevated concentrations of arsenic (As), cadmium (Cd), chromium (Cr), and lead (Pb) in soils and river sediments affected by mining activities, with consequent risks to crop safety and human health [4–10].

The toxicological properties of these PTEs are particularly relevant for agricultural workers, who may experience prolonged and repeated contact with contaminated soil and irrigation water, often without adequate protective measures. PTEs such as As are linked to skin lesions, neuropathies, and increased risks of skin, lung, and bladder cancers [11,12]. Cr(VI) is also recognized as a carcinogenic compound, while Cd and Pb are associated with renal dysfunction and neurotoxic effects, respectively, even at relatively low exposure levels [13,14]. These toxicological statements refer to general exposure to PTEs in contaminated environmental media and are commonly based on total concentrations reported in environmental studies [15,16].

In Ecuador, mining activity is concentrated along the southern Andean region, particularly in the provinces of El Oro, Azuay, Loja, and Zamora Chinchipe, where artisanal and small-scale gold mining (ASGM) has been historically developed and remains an important economic activity. Previous studies conducted in mining districts such as Ponce Enríquez and Santa Rosa have reported elevated concentrations of PTEs in soils, river sediments, and water bodies, frequently exceeding national and international environmental quality standards [2,17]. In Santa Rosa, mining activity is characterized by approximately 85 registered mining concessions covering around 300 km^2 [18], reflecting a high density of artisanal and small-scale mining activity, although many concessions remain in exploration or early development stages. More recently, investigations in mining-impacted watersheds of Santa Rosa have reported substantial metal(loid) enrichment in surface waters, highlighting the persistence of mining-derived contamination and its potential adverse effects on downstream aquatic ecosystems [19]. Within this regional context, the Santa Rosa canton (El Oro province) represents a particularly sensitive mining-agricultural interface, where agricultural activities coexist in close spatial proximity to mining operations and agricultural production depends heavily on irrigation systems that may be affected by upstream mining-derived contaminants. This evidence highlights the environmental pressure exerted by mining activities on agricultural landscapes and underscores the need for integrated assessments of contamination and risk, particularly those focused on soil and irrigation water quality in mining-influenced agricultural areas.

Despite growing evidence of environmental contamination in Santa Rosa, southern Ecuador, previous studies in Ecuadorian mining districts have primarily focused on the characterization of PTE concentrations in individual environmental compartments, particularly soils, river sediments, or surface waters. However, these studies have not integrated soils and irrigation water data within a unified framework to assess human health risks. Quantitative risk assessments addressing occupational exposure of agricultural workers in mining-impacted areas of southern Ecuador remain scarce. Therefore, this study addresses this gap by (i) determining the concentrations of PTEs in agricultural soils and irrigation water in a mining-influenced agricultural area of Santa Rosa, (ii) evaluating

contamination levels by comparing measured concentrations with Ecuadorian regulatory limits, and (iii) estimating non-carcinogenic and carcinogenic risks for adult agricultural workers through dermal exposure pathways using the U.S. EPA methodology. Dermal exposure was prioritized because it represents the most direct and continuous exposure route for agricultural workers in contact with contaminated soil and irrigation water during routine farming activities.

The results provide a comprehensive baseline for understanding environmental contamination and associated human health risks in a mining-impacted agricultural system, contributing to improved environmental monitoring through the control of priority pollutants in soils and irrigation water, risk management, and the development of preventive strategies in a region where mining and agriculture coexist.

2. Materials and Methods

2.1. Study Area

Santa Rosa canton is located in El Oro province, in the southern coastal region of Ecuador. It has an approximate population of 80,000 inhabitants [20], and covers a territorial area of 944.41 km^2. The climate is classified as humid tropical, with temperatures ranging from 18 °C to 26 °C and annual precipitation between 500 and 1000 mm, mainly concentrated from December to May [21]. Santa Rosa is situated on the Paleozoic Tahuín Group, composed of schists, phyllites, and gneisses, overlain by Quaternary alluvial and colluvial deposits of gravel, sand, and clay (Figure S1) [22–24].

Gold-mining activities in Santa Rosa began in 1985 and have continued uninterruptedly for nearly four decades, with operations concentrated in the upper part of the Santa Rosa River basin, near the El Panteon and Los Gringos tributaries. The mineralization corresponds to an epithermal gold-copper system, in which gold is hosted in hydrothermal breccias and quartz-arsenopyrite veins, with a mineral assemblage that includes pyrite, arsenopyrite, chalcopyrite, and native gold [25]. The release of PTEs into the environment is primarily associated with the oxidation of sulfide minerals, which generates acid mine drainage and mobilizes elements such as As, Cu, and Fe into soils and drainage systems, a process exacerbated by mining environmental liabilities and illegal mining operations identified in the area [19,26].

The study area consists of three cacao cultivation areas (CCN51 variety), covering approximately seven hectares (Figure 1). During the dry season, irrigation water is obtained from a canal supplied by the Santa Rosa River. In the rainy season, irrigation depends exclusively on precipitation.

2.2. Sample Collection

Soil sampling was conducted in June 2025 during the dry season. A total of 35 individual agricultural soil samples were collected and subsequently combined into 14 composite samples (SAG-01 to SAG-14), each representing two or three neighboring sampling points. In addition, 12 irrigation water samples were collected from the irrigation canal (WC-01 to WC-12).

For soil collection, sampling points were distributed within each previously delimited agricultural area considering site-specific characteristics, including terrain slope and proximity to water bodies [27]. At each sampling location, the surface litter layer and the upper 10 cm of soil were removed prior to sampling, and soil samples were collected from the 10–30 cm depth interval. This approach was adopted to minimize the influence of leaf litter and harvest residues, which are abundant in cacao plantations and continuously accumulate on the soil surface, potentially introducing variability that does not reflect the geochemical characteristics of the underlying soil. Approximately 1 kg of material was collected from each sampling point. The samples were dried under controlled temperature

conditions (≤30 °C) in a oven (CARBOLITE AX60, Carbolite Gero Ltd., Hope Valley, UK) and manually disaggregated. Following the methodology of ASTM International (2024), the disaggregated material was quartered to prepare the 14 composite samples to ensure representativeness, reduce soil spatial variability, and optimize the analytical process [28]. Each composite sample was sieved through a No. 20 mesh. Finally, the samples were quartered again to obtain approximately 50 g for analysis.

Water sampling in the irrigation canal was conducted in June and October 2025 during the dry season. Six samples of 500 mL were collected in each campaign. Sampling was restricted to the dry season due to the operational conditions of the irrigation system, as the opening of canal gates does not follow a fixed schedule, leading to uncertainty regarding water availability during other periods of the year. The sampling locations were selected to represent the canal reaches directly influencing the agricultural areas within the study site. Consequently, the collected samples provide a baseline characterization of water quality under the prevailing hydrological and operational conditions. The results should therefore be interpreted as a characterization of conditions at the time of sampling and are not intended to support seasonal or long-term assessments of water quality. Sampling was carried out following the protocols outlined in the National Field Manual for the Collection of Water-Quality Data of the U.S. Geological Survey (2006) [29]. The samples were collected in high-density polyethylene (HDPE) bottles. For preservation, they were acidified with concentrated HNO_3 to pH ≤ 2 and refrigerated at 2 °C to 5 °C [30].

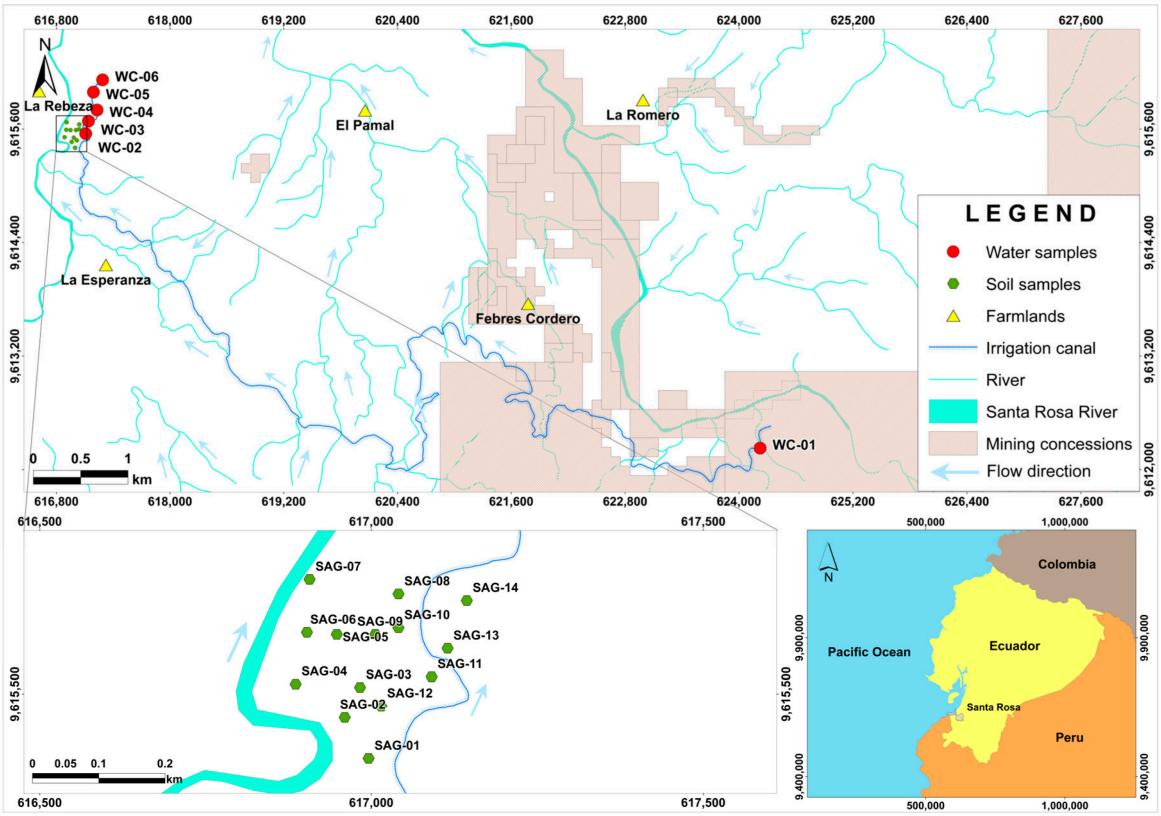


Figure 1. Location map of the study area and soil and water sampling points.

2.3. Physicochemical Parameters and PTE Concentration

In soil samples, pH and electrical conductivity (EC) were determined. pH was measured in a 1:2.5 soil-distilled water suspension (m:v), while EC was determined in a 1:5 soil-distilled water suspension (m:v). In water samples, pH, temperature, EC, total dissolved solids (TDS), and dissolved oxygen (DO) were measured. Physicochemical parameters

were determined in situ using a calibrated portable multiparameter probe (HACH HQ40D, Hach Sales and Service Canada LP, London, ON, Canada).

The concentrations of As, Cd, Cu, Cr, Ni, Pb, and Zn in soil samples were determined by X-ray fluorescence (ZSpec-EMax, ZSpec Inc., East Greenbush, NY, USA). The detection limits (mg/kg) were as follows: As = 0.2, Cd = 0.05, Cu = 0.5, Cr = 5, Ni = 1, Pb = 0.8, and Zn = 0.5. For quality assurance and quality control (QA/QC), the certified reference material NIST 2709a (San Joaquin Soil) was analyzed to assess method accuracy. Recoveries for all analyzed PTEs ranged from 92% to 115%. In water samples, the concentrations of PTEs were determined using ICP-MS (NexION 300D, Perkin Elmer, Waltham, MA, USA), at the University of Granada, Spain. Detection limits were below 0.0001 mg/L for all analyzed PTEs, while rates ranged from 90% to 105%. Analytical precision was assessed through replicate analyses, yielding relative standard deviations below 10% for all PTEs in both soil and water matrices.

2.4. Assessment of Agricultural Soil and Irrigation Water Quality

The concentrations of PTEs obtained from soil and water samples were compared with the Maximum Permissible Limits (MPLs) established in Ecuador's Unified Text of Secondary Environmental Legislation of the Ministry of Environment (TULSMA) (Table S1) [31,32]. For soil, the agricultural land-use quality criterion was applied, in accordance with the productive use of the evaluated farms, and for water, the agricultural or irrigation-use criterion was applied, considering the function of the sampled canal. Based on this comparison, the frequency and magnitude of exceedances in each matrix were determined, providing input for the subsequent human health risk assessment.

2.5. Human Health Risk Assessment

The human health risk assessment focused exclusively on the dermal exposure pathway, selected based on the occupational exposure scenario identified through field surveys. In the study area, agricultural activities such as soil preparation, planting, and harvesting involve frequent and prolonged direct contact with both soil and irrigation water, making dermal absorption the most relevant exposure route for agricultural workers. The ingestion and inhalation pathways were not considered in the assessment because they were not consistent with the occupational exposure conditions observed during field investigations. Furthermore, inhalation exposure was considered negligible, as the analyzed PTEs are non-volatile under ambient environmental conditions and the agricultural practices evaluated do not involve significant dust-generating activities. To characterize the exposed population, a census was conducted through field reconnaissance and direct consultation with potential receptors. A total of 28 active agricultural workers were identified, representing the entire population engaged in agricultural activities within the study area.

Risk assessment was based on the U.S. EPA methodology for calculating the potential absorbed dose through dermal contact with soil and water in agricultural settings. The Average Daily Dermal Dose (ADD_{dermal}) was calculated using Equations (1) and (2) for soil and water, respectively [15,16], integrating both the exposure parameters obtained from the surveys and the reference values established by the U.S. EPA (Table S2).

$$ADD_{dermal\text{-}soil} = \frac{C_{soil} \times SA \times AF \times ABS \times EF \times ED \times EV \times CF_1}{BW \times AT} \quad (1)$$

$$ADD_{dermal\text{-}water} = \frac{C_{water} \times SA \times Kp \times EF \times ED \times EV \times t_{event} \times CF_2}{BW \times AT} \quad (2)$$

where C_{soil} is the concentration of PTEs in soil (mg/kg); C_{water} is the concentration of PTEs in water (mg/L); SA is the exposed skin surface area (cm^2); AF is the adherence factor

($mg/cm^2 \cdot event$); ABS is the absorption factor; Kp is the dermal permeability coefficient (cm/h); EF is the exposure frequency (days/year); ED is the exposure duration (years); EV is the event frequency (events/day); t_{event} is the event duration (h/event); BW is the body weight (kg); AT is the averaging time (days); and CF_1 and CF_2 are the conversion factors.

Non-carcinogenic risk was estimated using the hazard quotient (HQ) (Equation (3)), which relates the Average Daily Dose (ADD) to the Reference Dose established for each element (RfD, mg/kg·day). This indicator allows determining whether exposure represents a potential health risk: HQ values < 1 indicate that the estimated dose is within the range considered safe, whereas values above 1 suggest the possible occurrence of systemic effects associated with the evaluated contaminant [15].

$$HQ = \frac{ADD}{RfD} \tag{3}$$

For the combined assessment of the risk posed by multiple contaminants, the hazard index (HI) (Equation (4)) was used. This index is obtained by summing the HQ values corresponding to each element for the dermal exposure route. The HI allows estimating the cumulative effect of several contaminants on human health. Under this approach, HI values < 1 indicate that combined exposure remains within the range considered safe, whereas values above 1 suggest a potential risk for the evaluated population [16].

$$HI = \sum_{i=1}^{n} HQ_i \tag{4}$$

For carcinogenic risk, the probability of a worker developing cancer over a lifetime (CR) was estimated according to exposure to each PTE (Equation (5)). This value depends on the ADD and the slope factor (SF; kg·day/mg), which represents the upper estimate of the increase in cancer risk associated with exposure to a unit dose of the carcinogenic agent [33].

$$CR = ADD \times SF \tag{5}$$

Subsequently, the obtained values were summed to calculate the Total Carcinogenic Risk (TCR) (Equation (6)). The following criteria were used for interpretation: when $TCR < 1 \times 10^{-6}$, the risk is negligible; when TCR ranges between 1×10^{-6} and 1×10^{-5}, the risk is low; when TCR is between 1×10^{-5} and 1×10^{-4}, the risk is tolerable and requires monitoring; and when $TCR > 1 \times 10^{-4}$, the risk is high and requires priority attention [33].

$$TCR = \sum_{i=1}^{n} TCR_i \tag{6}$$

Toxicity values (Table S3), specifically the RfD_{dermal} and SF_{dermal}, were obtained from the Risk Assessment Information System (RAIS) and are derived from oral reference values through the gastrointestinal absorption factor (ABS_{GI}) established by the U.S. EPA for each PTE [16]. Carcinogenic risk was estimated only for As, Cr, and Pb, as these were the only evaluated PTEs with a reported slope factor in the RAIS database [34]. The slope factor used for Cr corresponds to Cr(VI). Because only total Cr concentration was determined in this study, carcinogenic risk was estimated under the conservative assumption that all measured Cr was present as Cr(VI). This health-protective approach provides an upper-bound risk estimate and is consistent with commonly adopted practices when chromium speciation data are unavailable [35].

2.6. Statistical Analysis

The concentrations of PTEs measured in soil and water were analyzed using descriptive statistics to characterize data variability and provide context for their interpretation within the study area [36–38]. The associations between physicochemical parameters and PTE concentration in soil and water were analyzed using Spearman's correlation coefficient, considering correlations with $p < 0.05$ as significant [39,40]. Additionally, principal component analysis (PCA) was applied to standardized data to identify the covariance structure among variables and evaluate possible common contamination sources [41,42]. Elements with high loadings ($|\text{loading}| \geq 0.3$) within the same component were interpreted as indicators of a potential shared origin [43,44].

3. Results and Discussion

3.1. Physicochemical Properties of Soil and Water

Figure 2a,b summarize the behavior of the physicochemical parameters measured in agricultural soil and irrigation water, respectively. Overall, the results show that the soil exhibits slightly acidic conditions and low EC, suggesting no salinity-related limitations but potentially favorable conditions for the mobility of certain pH-sensitive PTEs [45].

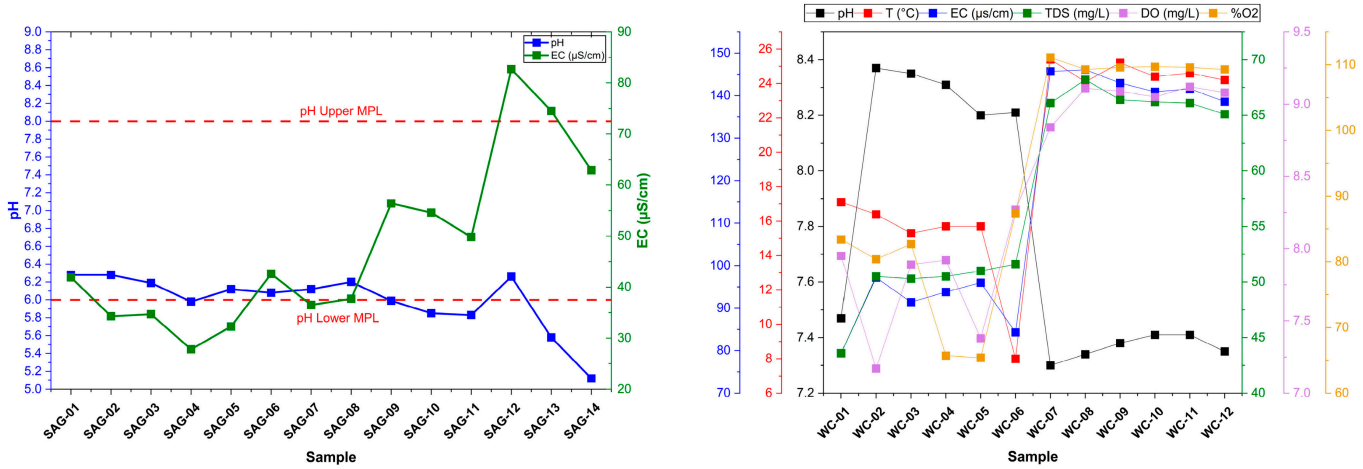


Figure 2. Physicochemical parameters: (**a**) soil samples; (**b**) water samples.

In soil, pH ranged from 5.12 to 6.28, indicating slightly to moderately acidic conditions in all 14 samples. Six samples were below the lower limit of the TULSMA reference range for agricultural soils (pH 6–8), with SAG-14 showing the lowest pH value. These slightly to moderately acidic conditions can enhance the mobility and bioavailability of cationic metals such as Cu, Pb, Zn, and Ni, since low pH reduces their adsorption to the solid phase [45]. In contrast, As, as an oxyanion, does not follow this trend: its mobility is governed mainly by sorption to Fe/Mn oxides and by redox conditions, so under the mildly acidic, oxic conditions of the study soils it tends to remain associated with these oxides [46]. On the other hand, EC ranged from 27.8 to 82.7 µS/cm, well below the permissible limit of 2000 µS/cm, indicating no salinity restrictions for agricultural use.

In water, pH ranged from 7.30 to 8.37, indicating neutral to slightly alkaline conditions in both sampling campaigns. The June 2025 campaign showed a wider range (7.47–8.37) than the October 2025 campaign (7.30–7.41). EC ranged from 79.4 to 146.1 µS/cm, with higher values in October 2025 (138.6–146.1 µS/cm) than in June 2025 (79.4–97.2 µS/cm), indicating a slight seasonal increase in mineralization. TDS followed the same trend (43.6–68.2 mg/L), while DO concentrations (7.17–9.12 mg/L) and saturation percentages

(65.4–111.1%) showed adequate oxygenation conditions in both periods. The slight increase in EC and TDS between the June and October campaigns suggests temporal variation in water chemistry, possibly associated with changes in flow rates and solute concentration during the dry season [47]. This should be monitored through longer-term programs to establish robust seasonal trends. All physicochemical parameters of the water complied with the TULSMA criteria for agricultural use.

3.2. Concentration of PTEs in Soil and Water

Table 1 presents the statistical summary of PTE concentration in soil and water samples. Figure 3 shows the spatial distribution of PTE concentration in soil compared with the TULSMA MPLs for agricultural use. As ranged from 11.36 to 53.05 mg/kg (p50: 28.36 mg/kg), exceeding the MPL of 12 mg/kg in 13 of the 14 analyzed samples (93%). In several samples, the concentration exceeded the standard by a factor of two to four. Cr showed a similar pattern, with values ranging from 63.72 to 153.40 mg/kg (p50: 98.10 mg/kg) and exceedances of its MPL of 65 mg/kg in 93% of the samples. Cu concentrations (31.46–87.81 mg/kg; p50: 64.04 mg/kg) exceeded the MPL of 63 mg/kg in eight samples (57%). Ni exceeded its threshold of 50 mg/kg in only two samples (14%), whereas Cd, Pb, and Zn remained below their respective MPLs in 100% of the samples. To complement this regulatory comparison, contamination factors (CF) were calculated as the ratio of the median concentration of each PTE to the corresponding world-average background value for soils reported by Kabata-Pendias [48], and classified according to Hakanson: CF < 1 (low), 1–3 (moderate), 3–6 (considerable), and ≥6 (very high) [49]. As showed the highest enrichment (CF = 6.03, very high), followed by Cu (4.57, considerable), Cr (2.34), Ni (2.17), Cd (1.22), and Zn (1.17), all within the moderate category, while Pb (0.88) corresponded to a low contamination level.

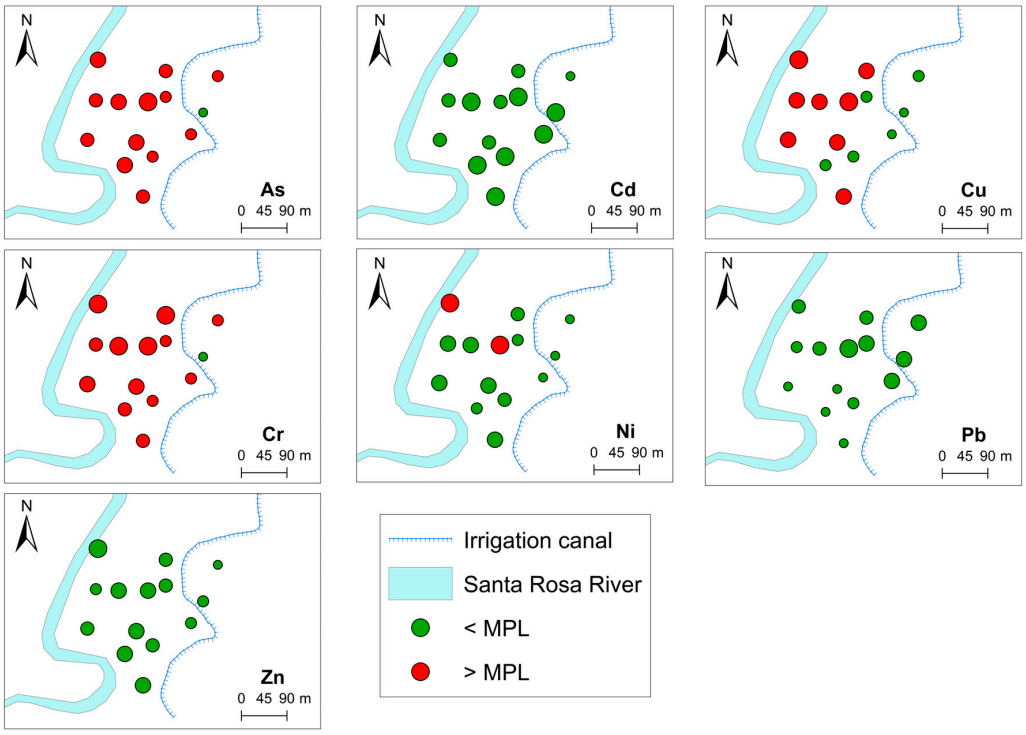


Figure 3. PTE concentrations in soil compared with the TULSMA environmental quality criterion. MPL = maximum permissible limit.

Table 1. Statistical summary of the concentration of PTEs in soil and water.

	Parameter	As (mg/kg)	Cd (mg/kg)	Co (mg/kg)	Cu (mg/kg)	Cr (mg/kg)	Mn (mg/kg)	Mo (mg/kg)	Ni (mg/kg)	Pb (mg/kg)	Zn (mg/kg)
Soil	MPL [1]	12	2	-	63	65	-	-	50	100	200
	Minimum	11.36	0.20	-	31.46	63.72	-	-	16.59	16.29	62.35
	p50 *	28.36	0.50	-	64.04	98.10	-	-	38.97	21.99	81.62
	p95 *	46.79	0.81	-	86.30	146.15	-	-	57.39	49.34	92.11
	Maximum	53.05	0.98	-	87.81	153.40	-	-	57.65	79.36	95.35
	SD	12.83	0.19	-	17.07	28.68	-	-	12.92	16.08	10.96
	Parameter	**As (µg/L)**	**Cd (µg/L)**	**Co (µg/L)**	**Cu (µg/L)**	**Cr (µg/L)**	**Mn (µg/L)**	**Mo (µg/L)**	**Ni (µg/L)**	**Pb (µg/L)**	**Zn (µg/L)**
Water	MPL [2]	100	10	50	2000	1000	200	10	200	50	2000
	Minimum	3.45	0.10	0.75	6.42	0.46	51.61	-	2.61	0.82	13.16
	p50 *	10.48	0.18	0.98	6.91	0.47	66.16	-	2.81	0.88	14.70
	p95 *	11.05	0.90	3.48	16.21	0.56	183.61	0.22	4.80	1.41	76.08
	Maximum	11.11	0.99	3.93	18.36	0.58	196.21	0.25	5.19	1.50	89.86
	SD	3.26	0.38	1.32	5.15	0.05	63.16	0.11	1.07	0.29	33.29

[1] MPLs (Maximum permissible limit) for contaminants in soil for agricultural use [32]. [2] MPLs for contaminants in water for agricultural or irrigation use [31]. * p50: 50th percentile/median. * p95: 95th percentile.

From a spatial perspective, As, Cr, and Cu exceedances were widespread across the study area rather than confined to specific zones, consistent with their high exceedance frequencies (93%), while Cu exceedances showed a less uniform distribution. This pattern likely reflects a diffuse contribution from regional mining-related and geogenic sources, although PTE distribution may also be influenced by the natural variability of parent material, soil physicochemical conditions, and local agricultural practices [48]. The greatest data dispersion was observed for Cr, Pb, and As, with standard deviations of 28.68, 16.08, and 12.83 mg/kg, respectively, indicating a heterogeneous distribution of these elements within the study area.

The widespread occurrence of As and Cr above the MPLs in the evaluated soils is consistent with contamination patterns reported in other mining-influenced areas of El Oro province [50,51]. The geological substrate of the study area includes a sulfide mineral association (pyrite, arsenopyrite, and chalcopyrite), whose oxidation under surface conditions may favor the release of As, Fe, and S into soils and drainage systems [52,53]. These elevated concentrations likely reflect both a geogenic component, from the natural weathering of this substrate, and a mining-related component, whereby decades of artisanal mining may have accelerated sulfide oxidation; their relative contributions cannot be separated here, as both share the same mineralogical origin and no direct source-tracing methods (isotopic or mineralogical) were applied. Similar geochemical mechanisms have been documented in soils and sediments from mining areas in Ponce Enríquez [17] and in other gold mining regions of Latin America [54,55]. Moreover, probabilistic assessments of agricultural soils influenced by gold mining similarly identified As as one of the dominant contaminants associated with sulfide-rich mineralization [1]. Comparable contamination patterns have also been documented in the Mantaro River basin (Peru) [56], where mining-related activities and ore-bearing geological formations contribute to the enrichment of trace elements in agricultural soils [57]. Similar geochemical processes have been reported in the Marmato gold district and the Sinú River Basin (Colombia), where artisanal gold mining and sulfide mineral oxidation promote the mobilization of potentially toxic elements into surrounding environmental matrices [58,59]. These regional comparisons suggest that the predominance of As, Cr, and Cu observed in Santa Rosa is consistent with contamination patterns commonly reported in Andean gold-mining environments.

Although Cu exceeded the MPL in 57% of the samples, the role of agrochemical inputs cannot be ruled out as a contributing factor. In the study area, cacao is the predominant crop and the use of agrochemicals was reported by local farmers during the field surveys;

copper-based fungicides are widely applied in Ecuadorian cacao cultivation to control moniliasis and black pod, and their repeated use may contribute to Cu accumulation in surface soils independently of mining-related sources [60]. Studies in cacao-growing regions without mining influence have reported elevated soil Cu attributable to the long-term use of copper-based fungicides: fungicide-treated cocoa soils have shown significantly higher Cu than adjacent untreated plots [61], with total Cu reaching 215–287 mg/kg in some cacao soils under repeated copper-fungicide application [62]. Ni exceeded the established limit in only 14% of the samples, while Cd, Pb, and Zn remained within the regulatory limits in all cases. This suggests that these elements may be less influenced by geogenic enrichment and anthropogenic inputs under the prevailing soil conditions.

Regarding the concentration of PTEs in irrigation water, all samples showed values below the TULSMA MPLs for agricultural use (Table 1). As ranged from 3.45 to 11.11 μg/L (MPL = 100 μg/L), Cd from 0.10 to 0.99 μg/L (MPL = 10 μg/L), and Pb from 0.82 to 1.50 μg/L (MPL = 50 μg/L). Mn recorded the highest absolute concentrations among the analyzed PTEs (51.61–196.21 μg/L), approaching the MPL of 200 μg/L at one sampling point, without exceeding it. Standard deviation (SD) was low for most PTEs, with notable exceptions for Mn (SD = 63.16 μg/L) and Zn (SD = 33.29 μg/L).

The Mn concentration approaching the regulatory limit was recorded exclusively at the sampling point located closest to the mining-influenced area, while the remaining samples showed concentrations well below the MPL. This localized pattern is consistent with a punctual contribution potentially associated with mining-related sources, rather than a generalized condition of the irrigation water in the study area. Although all values comply with current regulatory thresholds, the continued use of irrigation water with Mn concentrations approaching the MPL at specific points may represent a relevant aspect to consider in long-term water quality management and monitoring strategies for the agricultural area.

The compliance of all water samples with the MPLs contrasts with the soil results, consistent with the preferential partitioning of mining-derived PTEs into the solid phase rather than the dissolved phase. The proximity of Mn to the MPL nonetheless requires attention, given that the solubility of this PTE is sensitive to redox fluctuations that may occur during seasonal hydrological transitions [2,63].

3.3. Statistical Analysis

3.3.1. Spearman Correlation

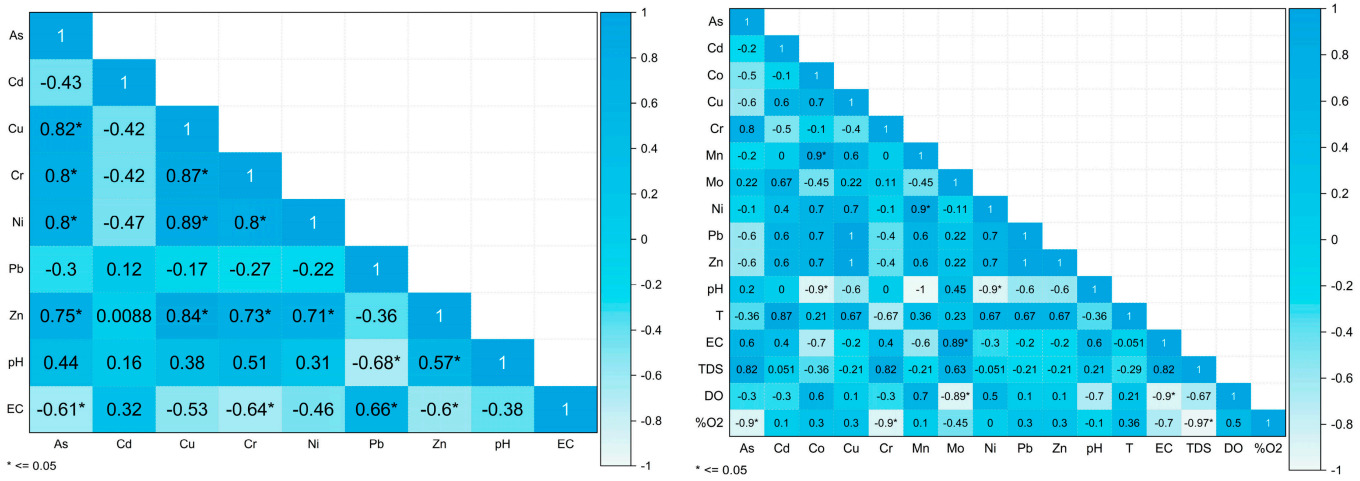
The Spearman correlation results showed three distinct association patterns among the PTEs and physicochemical parameters analyzed in soil samples (Figure 4a). The first group included As, Cu, Cr, Ni, and Zn, which showed strong and statistically significant positive correlations with each other (r_s = 0.71–0.89, $p < 0.05$). The most notable correlations were Cu-Cr (r_s = 0.87), Cu-Zn (r_s = 0.84), Cu-Ni (r_s = 0.89), and As-Cu (r_s = 0.82). This covariation pattern suggests that these PTEs may share a common origin, potentially associated with the sulfide mineralization of the geological substrate in the study area (chalcopyrite and arsenopyrite), whose oxidation under surface conditions may favor the simultaneous release of these elements into the soil [17,64]. However, correlation analysis alone is insufficient to establish definitive source attribution, and these interpretations should be considered as indicative rather than conclusive.

Cd did not show significant correlations with any of the PTEs or physicochemical parameters evaluated ($p > 0.05$ in all cases). This suggests an independent pattern of variation that may reflect a different source or geochemical behavior, possibly linked to agrochemicals such as phosphate fertilizers or fungicides [1].

Pb showed a distinct pattern compared with the geogenic group, with non-significant negative correlations with As, Cu, Cr, Ni, and Zn. However, it showed a significant negative correlation with pH ($r_s = -0.68$, $p < 0.05$) and a significant positive correlation with EC ($r_s = 0.66$, $p < 0.05$), suggesting that its spatial distribution in soil may be more strongly influenced by soil physicochemical properties than by the geogenic source influencing the other PTEs. This behavior is consistent with reports from soils in mining areas, where pH is a key factor regulating Pb mobility and availability [65]. Finally, the significant negative correlations of EC with As ($r_s = -0.61$), Cr ($r_s = -0.64$), and Zn ($r_s = -0.60$) suggest that, in areas with higher soil ionic strength, these elements tend to show lower mobility, probably due to precipitation or surface adsorption processes [41].

In water samples, the Spearman correlation showed fewer significant correlations than in soil (Figure 4b), which is consistent with the greater physicochemical homogeneity of irrigation water along the sampling canal. Co, Mn, and Ni showed positive correlations with each other, with the strongest correlations observed between Co-Mn ($r_s = 0.90$, $p < 0.05$) and Mn-Ni ($r_s = 0.90$, $p < 0.05$). Co and Ni also showed significant negative correlations with pH ($r_s = -0.90$, $p < 0.05$), suggesting that their availability in water may be strongly influenced by acidity conditions. This behavior is characteristic of redox-sensitive metals, whose solubility increases under conditions of higher acidity, a pattern widely documented in water systems affected by mine drainage [2]. This pattern is also consistent with previous hydrogeochemical observations in the Santa Rosa basin, where acidic conditions in mining-influenced tributaries have been associated with the mobilization of dissolved species [25].

Mo showed a significant positive correlation with EC ($r_s = 0.89$, $p < 0.05$) and a negative correlation with DO ($r_s = -0.89$, $p < 0.05$), suggesting that its concentration tends to increase under conditions of higher mineralization and lower water oxygenation, consistent with its geochemical behavior under reducing environments [66].



(**a**) (**b**)

Figure 4. Spearman correlation of physicochemical parameters and PTEs for (**a**) soil samples, and (**b**) water samples.

3.3.2. Principal Component Analysis (PCA)

The PCA applied to soil samples reduced the dimensionality of the original dataset of nine variables to three principal components with eigenvalues greater than 1, which together explained 88.20% of the total variance in the data (Table 2).

PC1 accounted for 57.42% of the variance and grouped As, Cu, Cr, Ni, and Zn with similar loadings (0.37–0.42), suggesting that a common factor, potentially associated with sulfide mineralization, may explain a substantial proportion of the distribution of PTEs

in soil. The larger variance explained by this component relative to the subsequent ones may suggest a greater influence of geogenic-related inputs, although PCA alone cannot quantify the relative contribution of geogenic versus anthropogenic sources [17,64]. PC2 explained an additional 16.99% of the variance, with dominant loadings for Pb (0.637) and negative loadings for pH (−0.487). This component may reflect a physicochemical control independent of the geogenic source, in which Pb mobility appears to be influenced by soil acid–base conditions [65]. PC3 accounted for the remaining 13.79%, with dominant loadings for Cd (0.639) and EC (0.451). The separation of Cd into an independent component, unrelated to both the mineralogical association of PC1 and the physicochemical control of PC2, supports the hypothesis of a different origin, potentially linked to agrochemical inputs such as phosphate fertilizers or fungicides used in local crops [1]. The suitability of the dataset for PCA was verified by a Kaiser-Meyer-Olkin measure of 0.66 and a statistically significant Bartlett's test of sphericity ($\chi^2 = 95.8$, $p < 0.001$), indicating acceptable sampling adequacy and sufficient inter-variable correlation for component extraction.

The PCA applied to water samples extracted three principal components with eigenvalues greater than 1, which together described 98.03% of the total variance (Table 2), indicating a well-defined covariance structure among the analyzed variables.

PC1 accounted for 67.21% of the variance, grouping most PTEs (Co, Cu, Mn, Ni, Pb and Zn) with positive loadings and pH, EC, TDS, and As with negative loadings. This configuration suggests that more than two-thirds of water variability may be explained by a single geochemical process, in which pH is the main regulator of PTEs mobility in the irrigation canal: under lower pH conditions, metal dissolution and availability tend to be favored, whereas As and TDS follow an opposite pattern [2]. PC2 explained an additional 18.77% of the variance, with dominant loadings for Cd (0.562) and Mo (0.524), along with a moderate contribution from temperature (0.296). The separation of Cd and Mo into a component independent from PC1 suggests that their variability may respond to a process different from pH control, possibly associated with anthropogenic inputs linked to agricultural practices and mobilization processes influenced by water temperature conditions [39]. PC3 accounted for the remaining 12.05% and was dominated by Cr (0.615), with significant negative loadings for $\%O_2$ (−0.445) and DO (−0.400). The inverse association between Cr and oxygenation parameters is consistent with its redox-sensitive behavior: under lower oxygenation conditions, Cr-bearing dissolved forms may be favored, while more oxidizing environments can promote precipitation or removal from the aqueous phase [66]. Due to the limited number of water samples relative to the number of variables analyzed, PCA for water was considered exploratory. Therefore, KMO and Bartlett's tests were not used as robust validation criteria, and PCA results were not interpreted as definitive evidence for source apportionment.

3.4. Human Health Risk Assessment

The results of the non-carcinogenic analysis indicate that dermal exposure to soil does not represent a relevant level of systemic risk for adult agricultural workers under the evaluated scenario (Table 3). The HI was 3.00×10^{-2}, a value considerably lower than the reference threshold of 1. However, the composition of the HI shows that risk was dominated by As and Cr, with contributions of 75.3% (HQ = 2.21×10^{-2}) and 22.9% (HQ = 6.72×10^{-3}), respectively. Together, these two PTEs accounted for 98.2% of the total index, whereas Cd, Ni, Pb, Cu, and Zn showed marginal contributions below 1.8%.

For dermal contact with water, the HI was 2.00×10^{-3}, also well below 1. The main contributors were As (HQ = 8.42×10^{-4}, ~42.2%) and Cd (HQ = 7.99×10^{-4}, ~40.0%), followed by Cr (~11.4%) and Mn (~4.7%). Together, these four PTEs accounted for approximately 98.3% of the total HI.

HI values for both matrices remained well below unity, indicating that non-carcinogenic systemic effects derived from dermal contact are unlikely under the evaluated occupational scenario. This finding is consistent with the results reported for mining-affected agricultural areas in Ponce Enríquez, where the dermal route contributed a smaller proportion of the total risk compared with ingestion and inhalation pathways [17]. The predominance of As and Cr in the HI calculation highlights the importance of these PTEs as priority contaminants for environmental monitoring, even when the aggregate risk levels remain within acceptable ranges. However, contrasting evidence has been reported in mining-impacted river systems in Peru, where Custodio et al. (2025) observed that As and Pb may exceed acceptable thresholds for both non-carcinogenic (HI > 1) and carcinogenic risk, particularly via direct contact with contaminated sediments [67]. These differences emphasize the strong influence of exposure route, population type, and environmental matrix on risk outcomes, and reinforce the need for site-specific risk assessment when interpreting contaminant impacts.

Table 2. PCA of physicochemical parameters and PTEs in soil and water samples.

Parameter	Soil			Water		
	PC1	PC2	PC3	PC1	PC2	PC3
As	0.40149	0.15166	0.07165	−0.3033	−0.04391	0.0493
Cd	−0.14654	−0.45125	0.63872	0.05921	0.56214	0.03464
Co	-	-	-	0.29871	−0.05665	0.11758
Cu	0.42226	0.12408	0.02433	0.30454	0.02158	0.02501
Cr	0.40299	0.08535	−0.1007	−0.08612	−0.23422	0.61529
Mn	-	-	-	0.26803	−0.10422	0.31243
Mo	-	-	-	−0.10492	0.52438	0.17004
Ni	0.40548	0.09765	0.14797	0.29947	−0.02328	0.13164
Pb	0.05012	0.63712	0.49689	0.29103	0.01351	0.20652
Zn	0.36995	−0.21119	0.24832	0.30467	0.00968	0.02755
pH	0.27941	−0.48712	0.20506	−0.30266	0.03573	−0.07411
T	-	-	-	0.24791	0.2958	0.09511
EC	−0.30784	0.23097	0.45128	−0.2892	0.10339	0.18756
TDS	-	-	-	−0.30191	−0.02352	0.08938
DO	-	-	-	0.13251	−0.39687	−0.40042
$\%O_2$	-	-	-	0.14019	0.28171	−0.445
Eigenvalues	5.16763	1.52941	1.24133	10.75381	3.00338	1.92804
Percentage of variance	57.42%	16.99%	13.79%	67.21%	18.77%	12.05%
Cumulative percentage	57.42%	74.41%	88.20%	67.21%	85.98%	98.03%

Table 3. Hazard quotient (HQ) and Hazard Index (HI) for dermal contact with soil and water.

PTEs	Soil		Water	
	HQ	HI	HQ	HI
As	2.21×10^{-2}	3.00×10^{-2}	8.42×10^{-4}	2.00×10^{-3}
Cd	3.13×10^{-4}		7.99×10^{-4}	
Co	-		1.14×10^{-5}	
Cu	4.41×10^{-6}		2.38×10^{-6}	
Cr	6.72×10^{-3}		2.27×10^{-4}	
Mn	-		9.28×10^{-5}	
Mo	-		6.62×10^{-8}	
Ni	1.22×10^{-4}		7.82×10^{-6}	
Pb	9.13×10^{-5}		1.25×10^{-5}	
Zn	3.84×10^{-7}		3.17×10^{-7}	

In the carcinogenic risk assessment, the TCR associated with dermal exposure to PTEs among agricultural workers was estimated (Table 4). For soil, the TCR was 4.34×10^{-5}, placing it within the tolerable range (1×10^{-5}–1×10^{-4}), which requires continuous monitoring. As dominated the carcinogenic risk profile, contributing 97.7% of the TCR

(CR = 4.24 × 10^{-5}); Cr contributed 2.2% (CR = 9.68 × 10^{-7}), and Pb contributed a negligible fraction (<0.001%). For water, the TCR was 1.65 × 10^{-6}, corresponding to a low risk level (1 × 10^{-6}–1 × 10^{-5}). Similar to the soil matrix, As was the dominant contributor (98.0%), followed by Cr at 2.0%, with Pb remaining negligible. In both matrices, As was confirmed as the main determinant of carcinogenic risk, and soil was the matrix of greatest concern for this outcome.

Table 4. CR and TCR for dermal contact with soil and water.

PTEs	Soil		Water	
	CR	TCR	CR	TCR
As	4.24 × 10^{-5}	4.34 × 10^{-5}	1.62 × 10^{-6}	1.65 × 10^{-6}
Cr	9.68 × 10^{-7}		3.27 × 10^{-8}	
Pb	3.26 × 10^{-10}		4.48 × 10^{-11}	

The almost exclusive contribution of As to the TCR is consistent with multi-route probabilistic assessments that identified the PTE as the main risk driver in Ecuadorian mining areas [17,68]. Comparable studies in other Ecuadorian regions impacted by gold mining have similarly reported low carcinogenic risk levels associated with water exposure under residential and recreational scenarios [69,70], which is consistent with the findings observed in this study for the irrigation canal. Similar observations have been reported in other Andean mining regions, including Peru [67] and Colombia [71,72], where As associated with sulfide-rich mineralization is the primary determinant of long-term carcinogenic risk. Although the estimated TCR in the present study remains within the tolerable range for soil and within the low-risk category for irrigation water, the predominance of As is consistent with a regional pattern characteristic of gold-mining environments across the Andes.

3.5. Implications for Environmental and Occupational Management

The results obtained provide a technical baseline to guide environmental and occupational management in agricultural areas influenced by mining activity. Excess levels of As, Cr, and Cu in soil suggest the need to implement periodic monitoring of PTEs in agricultural soils, as well as conducting assessments during both the dry and rainy seasons to identify potential seasonal variations. Although non-carcinogenic risk remained below the reference threshold, the dominant contribution of As to carcinogenic risk in soil indicates that this element should be considered a priority in future surveillance action.

From a preventive perspective, occupational control measures should be strengthened during agricultural activities, including the proper use of personal protective equipment, reduction in direct contact with wet or disturbed soils, hygiene practices after fieldwork, and training on PTE exposure pathways. In this way, the study provides useful information for decision-making in territories where mining and agricultural activities converge.

At the source, mitigating the influence of the mining area requires control of the oxidation of sulfide minerals that drive acid mine drainage and the mobilization of As, Cu, and Fe through the remediation of the mining environmental liabilities and stricter regulation of informal mining in the upper basin [19,26]. Regarding the soil matrix, although the estimated dermal health risk remained within tolerable limits, the exceedance of the MPLs by As, Cr, and Cu supported proportionate, targeted intervention rather than generalized remediation. For As, the dominant risk contributor, chemical immobilization using Fe-based amendments or biochar, which reduces As mobility and bioavailability, and assisted phytoremediation are among the most established and cost-effective options for agricultural soils [73,74]. The selection and scaling of such measures should be guided by prior site-specific characterization, including the speciation and spatially explicit studies identified above.

3.6. Limitations and Future Research

This study integrates environmental and occupational information to assess PTE-related risk in a mining-influenced agricultural area; nonetheless, several limitations should be acknowledged and define directions for future research. First, the assessment considered only the dermal pathway, consistent with the occupational scenario evaluated; incorporating incidental ingestion of soil particles, inhalation of resuspended dust, and consumption of crops grown in contaminated soils would allow a more comprehensive characterization of cumulative risk. Second, exposure parameters were treated as deterministic point estimates; probabilistic approaches such as Monte Carlo simulation would better capture the associated uncertainty [17]. Third, source identification relied on multivariate exploratory analysis; the application of direct source-tracing methods, such as mineralogical and isotopic analysis, would allow the geogenic and anthropogenic contributions to be apportioned conclusively.

A further priority is the experimental determination of the dermal bioaccessibility of PTEs in soils and irrigation, since the assessment relies on total concentrations and therefore yields conservative, upper-bound estimates. Recent studies in mining areas have shown that dermal bioaccessibility varies considerably among elements and material types, being generally low for As and higher for elements such as Pb and Zn [75]. The application of in vitro assays using synthetic sweat in the study area would allow site-specific absorption estimates to be obtained, refining the characterization of dermal risk and reducing the uncertainty associated with the use of total concentrations in human health risk assessment. Comparable evidence from the oral pathway in mining-affected matrices, with bioaccessibility values as low as ~8% for As [55], further indicates that the bioaccessible fraction is considerably lower than the total content. In the same direction, determining the speciation of the Cr(III)/Cr(VI) distribution would refine the carcinogenic risk estimate, which was based on total Cr under a conservative Cr(VI) assumption. Finally, the water results correspond to a single dry-season campaign; multi-season monitoring would capture the temporal variability of PTE concentrations, particularly for Mn, whose solubility is sensitive to redox fluctuations across hydrological seasons.

4. Conclusions

This study integrated soil and irrigation water quality data with a quantitative human health risk assessment in a mining-influenced agricultural area of the Santa Rosa canton, southern Ecuador.

The results revealed significant PTE accumulation in soils, with As and Cr exceeding the maximum permissible limits in 93% of the samples and Cu in 57%, with maximum concentrations reaching approximately 4.4, 2.4, and 1.4 times the respective limits for As, Cr, and Cu, identifying these elements as the principal contaminants of environmental concern. In contrast, PTE concentrations in irrigation water remained within the regulatory limits for agricultural use, although Mn concentrations approached the permissible threshold.

Human health risk assessment indicated that, under the dermal exposure scenario, contaminated soils did not indicate significant non-carcinogenic risks (HI = 3.00×10^{-2}), while the carcinogenic risk (TCR = 4.34×10^{-5}) remained within the tolerable range requiring monitoring, with As identified as the main contributor (~97.7%).

For dermal exposure to water, the non-carcinogenic risk also remained below the threshold (HI = 2.00×10^{-3}), while the carcinogenic risk (TCR = 1.65×10^{-6}) corresponded to a low risk on the basis of the same scale (10^{-6}–10^{-5}), again mainly controlled by As (~98.0%). Overall, the results indicate that As was the main element associated with risk under the evaluated scenario, and soil is the most relevant matrix for the carcinogenic

component, while water maintained low carcinogenic risk and non-carcinogenic risk below the established threshold.

These findings apply specifically to the dermal exposure pathway and should not be interpreted as an estimate of total human health risk; characterizing the latter would require a multi-pathway assessment incorporating incidental ingestion, dust inhalation, and dietary intake from crops.

Despite these limitations, the integrated approach adopted in this study, which links soil and water quality data with a quantitative human health risk assessment under an occupational dermal exposure scenario, provides a reproducible framework for similar mining–agriculture interface contexts in Ecuador and the Andean region in general. Since As was the dominant risk contributor, it represents a clear target for monitoring source-control actions, whereas, for the dermal exposure evaluated, the regulatory compliance of irrigation water indicates that the canal does not currently represent an acute chemical risk for agricultural activities.

Supplementary Materials: The following supporting information can be downloaded at: https://www.mdpi.com/article/10.3390/resources15060081/s1, Figure S1: Geological map of the study area; Table S1: Maximum permissible limits (MPLs) for contaminants in soil and water for agricultural or irrigation use.; Table S2: Exposure factors used in the human health risk assessment; Table S3: Toxicity values of PTEs.

Author Contributions: Conceptualization, J.G.-M., C.H.B.-T. and K.E.-S.; methodology, J.G.-M., C.H.B.-T. and S.J.-O.; software, J.G.-M.; validation and formal analysis, J.G.-M., C.H.B.-T. and K.E.-S.; investigation and data curation, J.G.-M., C.H.B.-T. and B.S.-A.; writing—original draft preparation, J.G.-M., C.H.B.-T. and B.S.-A.; writing—review and editing, G.M.-G., S.J.-O. and K.E.-S.; supervision, S.J.-O. and K.E.-S. All authors have read and agreed to the published version of the manuscript.

Funding: This research received no external funding.

Data Availability Statement: The data supporting the findings of this study are available upon reasonable request from the authors.

Acknowledgments: The authors gratefully acknowledge the laboratories of the Faculty of Engineering in Earth Sciences at ESPOL Polytechnic University for providing access to their facilities and analytical equipment, as well as for their technical support during sample preparation and analysis. The authors also thank Alberto Molinero-García, from the University of Granada, for his support with the ICP-MS analysis of the water samples. Finally, the authors thank ESPOL Polytechnic University for its institutional support throughout the development of this study.

Conflicts of Interest: The authors declare no conflicts of interest.

Abbreviations

The following abbreviations are used in this manuscript:

PTEs	Potentially toxic elements
As	Arsenic
Cd	Cadmium
Co	Cobalt
Cr	Chromium
Cu	Copper
Mn	Manganese
Mo	Molybdenum
Ni	Nickel
Pb	Lead
Zn	Zinc
EC	Electrical conductivity

TDS	Total dissolved solids
DO	Dissolved oxygen
XRF	X-ray fluorescence
ICP-MS	Inductively coupled plasma mass spectrometry
HDPE	High-density polyethylene
HNO_3	Nitric acid
NIST	National Institute of Standards and Technology
TULSMA	Unified Text of Secondary Environmental Legislation of the Ministry of Environment
MPL	Maximum permissible limit
HHRA	Human health risk assessment
ADD	Average daily dose
RfD	Reference dose
ABS_{GI}	Absorbed fraction in the gastrointestinal tract
HQ	Hazard quotient
HI	Hazard index
SF	Slope factor
CR	Cancer risk
TCR	Total cancer risk
RAIS	Risk Assessment Information System
U.S. EPA	United States Environmental Protection Agency
ASTM	American Society for Testing and Materials
ASGM	Artisanal and small-scale gold mining
USGS	United States Geological Survey
PCA	Principal component analysis
SD	Standard deviation
p50	50th percentile/median
p95	95th percentile
SA	Exposed skin surface area
AF	Adherence factor
ABS	Absorption factor
Kp	Dermal permeability coefficient
EF	Exposure frequency
ED	Exposure duration
EV	Event frequency
t_{event}	Event duration
BW	Body weight
AT	Averaging time
CF	Conversion factor
SAG	Agricultural soil sample code
WC	Water canal sample code
CCN51	Cacao cultivar code

References

1. Romero-Crespo, P.; Jiménez-Oyola, S.; Salgado-Almeida, B.; Zambrano-Anchundia, J.; Goyburo-Chávez, C.; González-Valoys, A.; Higueras, P. Trace Elements in Farmland Soils and Crops, and Probabilistic Health Risk Assessment in Areas Influenced by Mining Activity in Ecuador. *Environ. Geochem. Health* **2023**, *45*, 4549–4563. [CrossRef] [PubMed]
2. Jiménez-Oyola, S.; Valverde-Armas, P.E.; Romero-Crespo, P.; Capa, D.; Valdivieso, A.; Coronel-León, J.; Guzmán-Martínez, F.; Chavez, E. Heavy Metal(Loid)s Contamination in Water and Sediments in a Mining Area in Ecuador: A Comprehensive Assessment for Drinking Water Quality and Human Health Risk. *Environ. Geochem. Health* **2023**, *45*, 4929–4949. [CrossRef] [PubMed]
3. Tong, L.; Yang, A.; Fan, M.; Zheng, D.; Li, J.; Liu, H.; Li, C.; Tang, Y.; Cheng, L. Assessment of Heavy Metal Sources and Health Risks in Soil-Crop Systems of Fragmented Farmland. *Front. Public Health* **2025**, *13*, 1637595. [CrossRef] [PubMed]

4. Liu, X.; Chen, S.; Yan, X.; Liang, T.; Yang, X.; El-Naggar, A.; Liu, J.; Chen, H. Evaluation of Potential Ecological Risks in Potential Toxic Elements Contaminated Agricultural Soils: Correlations between Soil Contamination and Polymetallic Mining Activity. *J. Environ. Manag.* **2021**, *300*, 113679. [CrossRef] [PubMed]
5. Rouhani, A.; Gutiérrez, M.; Newton, R.A.; Al Souki, K.S. An Overview of Potentially Toxic Element Pollution in Soil around Lead–Zinc Mining Areas. *Environ. Rev.* **2025**, *33*, 1–16. [CrossRef]
6. Hu, B.; Shao, S.; Ni, H.; Fu, Z.; Huang, M.; Chen, Q.; Shi, Z. Assessment of Potentially Toxic Element Pollution in Soils and Related Health Risks in 271 Cities across China. *Environ. Pollut.* **2021**, *270*, 116196. [CrossRef] [PubMed]
7. Escot-Espinoza, V.M.; Rodríguez-Márquez, S.; Briseño-Bugarín, J.; López-Luna, M.A.; Flores de la Torre, J.A. Presence of Potentially Toxic Elements in Historical Mining Areas in the North-Center of Mexico and Possible Bioremediation Strategies. *Toxics* **2024**, *12*, 813. [CrossRef] [PubMed]
8. Li, W.; Cao, X.; Hu, Y.; Cheng, H. Source Apportionment and Risk Assessment of Heavy Metals in Agricultural Soils in a Typical Mining and Smelting Industrial Area. *Sustainability* **2024**, *16*, 1673. [CrossRef]
9. Sun, X.; Wang, B.; Li, Z. Pollution Status, Risk Assessment, and Source Identification of Heavy Metals in Farmland Topsoil of Mining Area Along the Yangtze River, East China. *Agriculture* **2025**, *15*, 2181. [CrossRef]
10. Rodrigues, F.H.S.; da Silveira Pereira, W.V.; Dias, Y.N.; Ramos, S.J.; Ribeiro, P.G.; Soares, M.B.; Pereira, M.F.; Fernandes, A.R. Environmental Impacts of Toxic Elements on Crop-Grazing Soils in Areas Surrounding Artisanal Mining in the Brazilian Amazon. *Environ. Geochem. Health* **2026**, *48*, 131. [CrossRef] [PubMed]
11. Zhou, Q.; Xi, S. A Review on Arsenic Carcinogenesis: Epidemiology, Metabolism, Genotoxicity and Epigenetic Changes. *Regul. Toxicol. Pharmacol.* **2018**, *99*, 78–88. [CrossRef] [PubMed]
12. IARC. *Arsenic, Metals, Fibres and Dusts*; International Agency for Research on Cancer: Lyon, France, 2012; Volume 100C.
13. Akter, F.; Das, S.; Sharmin, T.; Tahsin, M.R.; Amran, M.S.; Aktar, F. A Comprehensive Review on the Health & Ecological Impacts of Chromium, Cadmium and Lead Contamination. *J. Adv. Med. Pharm. Sci.* **2025**, *27*, 75–91. [CrossRef]
14. Tchounwou, P.B.; Yedjou, C.G.; Patlolla, A.K.; Sutton, D.J. Heavy Metal Toxicity and the Environment. In *Molecular, Clinical and Environmental Toxicology*; Luch, A., Ed.; Springer Nature Link: Berlin/Heidelberg, Germany, 2012; Volume 3, pp. 133–164.
15. U.S. EPA. *Risk Assessment Guidance for Superfund: Volume III-Part A, Process for Conducting Probabilistic Risk Assessment*; U.S. EPA: Washington, DC, USA, 2001.
16. U.S. EPA. *Risk Assessment: Guidance for Superfund Volume I: Human Heatlh Evaluation Manual (Part E, Supplemental Guidance for Dermal Risk Assessment) Final*; U.S. EPA: Washington, DC, USA, 2004.
17. Jiménez-Oyola, S.; Chavez, E.; García-Martínez, M.-J.; Ortega, M.F.; Bolonio, D.; Guzmán-Martínez, F.; García-Garizabal, I.; Romero, P. Probabilistic Multi-Pathway Human Health Risk Assessment Due to Heavy Metal(Loid)s in a Traditional Gold Mining Area in Ecuador. *Ecotoxicol. Environ. Saf.* **2021**, *224*, 112629. [CrossRef] [PubMed]
18. ARCERNNR. Geoportal: Catastro Minero. Available online: https://arcmineria.maps.arcgis.com/apps/webappviewer/index.html?id=27bfda03ce4342b3834a27010da857e5 (accessed on 6 June 2026).
19. Goyburo-Chávez, C.; Villamar-Marazita, K.; Aguilar-Aguilar, C.; Gonzalez-Valoys, A.; Jiménez-Oyola, S. Spatial and Temporal Distribution of Potentially Toxic Elements and Human Health Risk Assessment in the Gold Mining Area of Santa Rosa, Southern Ecuador. *Discov. Appl. Sci.* **2025**, *7*, 941. [CrossRef]
20. INEC. VIII Censo de Población y VII de Vivienda, 2022. Available online: https://www.censoecuador.gob.ec/resultados-censo/#resultados (accessed on 25 November 2025).
21. INAMHI. Visor de Estaciones Meteorológicas e Hidrológicas. Available online: https://inamhi.gob.ec/visor/visor (accessed on 14 January 2026).
22. Bristow, C.; Hoffstetter, R. *Léxico Estratigráfico Internacional*, 2nd ed.; Centre National de la Recherche Scientifique: Paris, France, 1977.
23. Feininger, T. *Geología de la Zona Arenillas-Puyango*; FAO AGRIS: Rome, Italy, 1975.
24. Kennerley, J.B. *Geology of Loja Province, Southern Ecuador*; IGS Photogeological Unit: London, UK, 1973.
25. Villamar-Marazita, K.; Goyburo-Chávez, C.; Valverde-Armas, P.E.; Vitvar, T.; Čech, P.; Michalko, J.; Jiménez-Oyola, S. Hydrochemistry and Isotopic Characterization of Water Resources in Santa Rosa Mining Area, Ecuador. *Groundw. Sustain. Dev.* **2025**, *31*, 101556. [CrossRef]
26. Angamarca, D.; Valarezo, L. *Determinación de la Contaminación del Recurso Hídrico Provocado Por la Actividad Minera en la Cuenca Alta del Río Santa Rosa, Provincia de el Oro*; Universidad Politécnica Salesiana: Cuenca, Ecuador, 2020.
27. Jiménez Ballesta, R. *Introducción a la Contaminación de Suelos*, 1st ed.; Mundi-Prensa: Madrid, Spain, 2017.
28. *ASTM C702/C702M-24*; ASTM International Standard Practice for Reducing Samples of Aggregate to Testing Size. ASTM International: West Conshohocken, PA, USA, 2024.
29. U.S. Geological Survey. *National Field Manual for the Collection of Water-Quality Data*; U.S. Geological Survey: Reston, VA, USA, 2006.
30. *NTE INEN 2169:2013*; Agua. Calidad del agua. Muestreo. Manejo y Conservación de Muestras. INEN: Quito, Ecuador, 2013.
31. Ministerio del Ambiente. *Anexo 1 del Libro VI—Norma de Calidad Ambiental y de Descarga de Efluentes: Recurso Agua*; Ministerio del Ambiente: Quito, Ecuador, 2017.

32. Ministerio del Ambiente. *Anexo 2 del Libro VI—Norma de Calidad Ambiental del Recurso Suelo y Criterios de Remediación Para Suelos Contaminados*; Ministerio del Ambiente: Quito, Ecuador, 2017.
33. U.S. EPA. *Guidelines for Carcinogen Risk Assessment*; U.S. EPA: Washington, DC, USA, 2005.
34. U.S. DOE. *RAIS: Risk Assessment Information System*; U.S. DOE: Washington, DC, USA, 2025.
35. Xu, S.; Yu, C.; Wang, Q.; Liao, J.; Liu, C.; Huang, L.; Liu, Q.; Wen, Z.; Feng, Y. Chromium Contamination and Health Risk Assessment of Soil and Agricultural Products in a Rural Area in Southern China. *Toxics* **2022**, *11*, 27. [CrossRef] [PubMed]
36. Daniel, W.W.; Cross, C.L. *Biostatistics: A Foundation for Analysis in the Health Sciences*; Décima.; Wiley: Hoboken, NJ, USA, 2013.
37. Triola, M.F. *Estadística*, 9th ed.; Pearson Educación: London, UK, 2004.
38. Kaur, P.; Stoltzfus, J.; Yellapu, V. Descriptive Statistics. *Int. J. Acad. Med.* **2018**, *4*, 60. [CrossRef] [PubMed]
39. Songara, Y.; Singhal, A.; Garg, R.D.; Rallapalli, S. Hydro-Chemical Profiling and Contaminant Source Identification in Agricultural Canals Using Data Driven Clustering Approaches. *Sci. Rep.* **2025**, *15*, 24806. [CrossRef] [PubMed]
40. Yang, Z.; Yu, J.; Yang, K.; Zhang, Q.; Chen, Y.; Qiao, S. Source Apportionment and Risk Assessment of Potentially Toxic Elements Based on PCA and PMF Model in Black Soil Area of Hailun City, Northeast China. *Toxics* **2024**, *12*, 683. [CrossRef] [PubMed]
41. Chen, S.; Wang, H.; Han, R. Source Apportionment of Potentially Toxic Elements in Agricultural Soils of Yingtan City, Jiangxi Province, China: A Principal Component Analysis–Positive Matrix Factorization Method. *Toxics* **2025**, *13*, 267. [CrossRef] [PubMed]
42. Liu, J.; Gong, C.; Ba, Y.; Liu, S.; Wan, H.; Zhao, X.; Li, Z.; Liu, X.; Yang, Z. Risk Assessment and Correlation Analysis of Potentially Toxic Element Pollution in Soil and Crops: A Case Study in a Typical Area. *Toxics* **2025**, *13*, 554. [CrossRef] [PubMed]
43. Liu, C.-W.; Lin, K.-H.; Kuo, Y.-M. Application of Factor Analysis in the Assessment of Groundwater Quality in a Blackfoot Disease Area in Taiwan. *Sci. Total Environ.* **2003**, *313*, 77–89. [CrossRef] [PubMed]
44. Hair, J.F.; Black, W.C.; Babin, B.J.; Anderson, R.E. *Multivariate Data Analysis*, 8th ed.; Cengage: Boston, MA, USA, 2019.
45. Kicińska, A.; Pomykała, R.; Izquierdo-Diaz, M. Changes in Soil and Mobility of Heavy Metals in Contaminated Soils. *Eur. J. Soil Sci.* **2022**, *73*, e13203. [CrossRef]
46. Bowell, R.J. Sorption of Arsenic by Iron Oxides and Oxyhydroxides in Soils. *Appl. Geochem.* **1994**, *9*, 279–286. [CrossRef]
47. Tohouri, P.; Adja, M.G.; Soro, S.I. Spatio-Seasonal Variability of Surface Water Mineralization in the Bonoua Region, Southeastern Côte d'Ivoire. *Front. Water* **2026**, *8*, 1795536. [CrossRef]
48. Kabata-Pendias, A. *Trace Elements in Soils and Plants*, 4th ed.; CRC Press—Taylor & Francis Group: Boca Raton, FL, USA, 2011.
49. Hakanson, L. An Ecological Risk Index for Aquatic Pollution Control. A Sedimentological Approach. *Water Res.* **1980**, *14*, 975–1001. [CrossRef]
50. Capa, D.; Valdivieso, A. *Categorización y Gestión del Riesgo Asociado a la Presencia de Metales Pesados Producto de las Actividades Extractivas en el Santa Rosa, El Oro*; Escuela Superior Politécnica del Litoral: Guayaquil, Ecuador, 2021.
51. Oviedo-Anchundia, R.; Moína-Quimí, E.; Naranjo-Morán, J.; Barcos-Arias, M. Contaminación por metales pesados en el sur del Ecuador asociada a la actividad minera. *Bionatura* **2017**, *2*, 437–441. [CrossRef]
52. Guzmán, F. *Evaluación de la Peligrosidad de los Elementos Potencialmente Tóxicos Presentes en Residuos Mineros Abandonados*; Universidad Politécnica de Madrid: Madrid, Spain, 2022.
53. Escobar-Segovia, K.; Jimenez-Oyola, S.; Garces-Leon, D.; Paz-Barzola, D.; Chavez Navarrete, E.; Romero-Crespo, P.; Salgado, B. Heavy Metals in Rivers Affected by Mining Activities in Ecuador: Pollution and Human Health Implications. In *Proceedings of the Sustainable Water Resources Management XI*; WIT Press: Southampton, UK, 2021; pp. 61–72.
54. Reyes, Y.C.; Vergara, I.; Torres, O.E.; Díaz, M.; González, E.E. Contaminación por metales pesados: Implicaciones en salud, ambiente y seguridad alimentaria. *Rev. Ing. Investig. Desarro.* **2016**, *16*, 66–77. [CrossRef]
55. González-Valoys, A.C.; Jiménez-Oyola, S.; Patinha, C.; García-Noguero, E.M.; Peco, J.; Segundo, F.; Barquero, J.I.; Vargas-Lombardo, M.; Esbrí, J.M.; Higueras, P. Oral Bioaccessibility and Probabilistic Human Health Risk Assessment of Potentially Toxic Elements in Stream Sediments from an Abandoned Gold Mine in Panama. *Environ. Geochem. Health* **2025**, *47*, 224. [CrossRef] [PubMed]
56. Custodio, M.; Peñaloza, R.; Espinoza, C.; Peralta-Ortiz, T.; Ordinola-Zapata, A.; Sánchez-Suárez, H.; Vieyra-Peña, E. Data on the Concentration of Heavy Metals and Metalloids in Lotic Water of the Mantaro River Watershed and Human Risk Assessment, Peru. *Data Brief* **2020**, *30*, 105493. [CrossRef] [PubMed]
57. Ccopi, D.; Requena-Rojas, E.; Ortega, K.; Solórzano-Acosta, R.; Révolo-Acevedo, R.; Pizarro, S. Bioaccumulation of Heavy Metals in High Andean Crops of the Peruvian Andes: Comparative Evaluation between Irrigated and Dry Systems. *J. Agric. Food Res.* **2026**, *25*, 102575. [CrossRef]
58. Torrance, K.W.; Redwood, S.D.; Cecchi, A. The Impact of Artisanal Gold Mining, Ore Processing and Mineralization on Water Quality in Marmato, Colombia. *Environ. Geochem. Health* **2021**, *43*, 4265–4282. [CrossRef] [PubMed]
59. Marrugo-Negrete, J.; Pinedo-Hernández, J.; Díez, S. Assessment of Heavy Metal Pollution, Spatial Distribution and Origin in Agricultural Soils along the Sinú River Basin, Colombia. *Environ. Res.* **2017**, *154*, 380–388. [CrossRef] [PubMed]

60. Torres, S.; Yadaicela, J.; Lascano, A.; Pilaloa, W. Eficacia comparativa de oxicloruro de cobre y sulfato de cobre pentahidratado en el control de Moniliophthora roreri en cacao (*Theobroma cacao* L.). *Polo Conoc.* **2026**, *11*, 1227–1243.
61. Azeez, M.O.; Adesanwo, O.O.; Adepetu, J.A. Effects of Copper Fungicides Spray on Nutrient Contents in Soils of Cocoa Growing Areas of Southwestern Nigeria. *Tanzan. J. Sci.* **2021**, *47*, 1546–1559. [CrossRef]
62. Kakutey, K.; Sackey, L.N.A.; Akoto, O. Impact of Accumulation of Copper from Application of Copper-Based Fungicides on Soil Properties in Ghana. *Discov. Environ.* **2023**, *1*, 1. [CrossRef]
63. Bartoszek, L.; Gruca-Rokosz, R.; Pękala, A.; Czarnota, J. Heavy Metal Accumulation in Sediments of Small Retention Reservoirs—Ecological Risk and the Impact of Humic Substances Distribution. *Resources* **2022**, *11*, 113. [CrossRef]
64. Li, X.; Tang, Y.; Wang, X.; Song, X.; Yang, J. Heavy Metals in Soil around a Typical Antimony Mine Area of China: Pollution Characteristics, Land Cover Influence and Source Identification. *Int. J. Environ. Res. Public Health* **2023**, *20*, 2177. [CrossRef] [PubMed]
65. Asare, M.O.; Száková, J.; Tlustoš, P. Mechanisms of As, Cd, Pb, and Zn Hyperaccumulation by Plants and Their Effects on Soil Microbiome in the Rhizosphere. *Front. Environ. Sci.* **2023**, *11*, 1157415. [CrossRef]
66. Wang, J.; Zhang, H.; Liu, J.; Hu, S.; Shi, J.; Li, X.; Song, D.; Niu, X. Distribution Characteristics, Source Identification, and Health Risk Assessment of Heavy Metals in Surface Water and Groundwater: A Case Study in Mining-Affected Areas. *Front. Water* **2025**, *7*, 1639009. [CrossRef]
67. Custodio, M.; Pizarro, S.; Huarcaya, J.; Ortega, K.; Ccopi, D. Ecological and Human Health Risk Assessment of Heavy Metals in Mining-Affected River Sediments in the Peruvian Central Highlands. *Toxics* **2025**, *13*, 783. [CrossRef] [PubMed]
68. Galarza, E.; Moulatlet, G.M.; Rico, A.; Cabrera, M.; Pinos-Velez, V.; Pérez-González, A.; Capparelli, M.V. Human Health Risk Assessment of Metals and Metalloids in Mining Areas of the Northeast Andean Foothills of the Ecuadorian Amazon. *Integr. Environ. Assess. Manag.* **2023**, *19*, 706–716. [CrossRef] [PubMed]
69. Passarelli, I.; Mora-Silva, D.; Jimenez-Gutierrez, M.; Logroño-Naranjo, S.; Hernández-Allauca, D.; Valdez, R.U.; Avalos Peñafiel, V.G.; Tierra Pérez, L.P.; Sanchez-Salazar, M.; Tobar Ruiz, M.G.; et al. Hg Pollution in Groundwater of Andean Region of Ecuador and Human Health Risk Assessment. *Resources* **2024**, *13*, 84. [CrossRef]
70. Passarelli, I.; Mora-Silva, D.; Arguello Guadalupe, C.; Carrillo Arteaga, T.; Ureta Valdez, R.; Orna Puente, L.M.; Tobar Ruiz, M.G.; Ati-Cutiupala, G.; Sanchez-Salazar, M.; Straface, S.; et al. Risks to Human Health from the Consumption of Water from Aquifers in Gold Mining Areas in the Coastal Region of Ecuador. *Resources* **2024**, *13*, 53. [CrossRef]
71. Salazar, J.P.; Saldarriaga, J.F.; Zapata, D.; López, J.E. Determination of Bioavailability, Potential Ecological and Human Health Risks, and Biomonitoring of Potential Toxic Elements in Gold Mine Tailings from Four Areas of Antioquia, Colombia. *Water Air Soil Pollut.* **2024**, *235*, 122. [CrossRef]
72. López, J.E.; Marín, J.F.; Saldarriaga, J.F. Assessing Pollution Degree and Human Health Risks from Hazardous Element Distribution in Soils near Gold Mines in a Colombian Andean Region: Correlation with Phytotoxicity Biomarkers. *Chemosphere* **2024**, *361*, 142471. [CrossRef] [PubMed]
73. Wan, X.; Lei, M.; Chen, T. Review on Remediation Technologies for Arsenic-Contaminated Soil. *Front. Environ. Sci. Eng.* **2020**, *14*, 24. [CrossRef]
74. Huslina, F.; Khudur, L.S.; Shah, K.; Surapaneni, A.; Netherway, P.; Ball, A.S. Mine Site Restoration: The Phytoremediation of Arsenic-Contaminated Soils. *Environments* **2024**, *11*, 99. [CrossRef]
75. Ferri-Moreno, I.; Martínez-del-Pozo, I.; Huertas, P.; Higueras, P.; Barquero-Peralbo, J.I.; Esbrí, J.M.; García-Lorenzo, M.L. Dermal Bioaccessibility and Health Risk Assessment Associated with Mining Production of Metals (Pb-Zn-Ag) and Critical Raw Materials (Sb-W) in the Iberian Peninsula. *Environ. Chem. Ecotoxicol.* **2025**, *7*, 506–515. [CrossRef]

Disclaimer/Publisher's Note: The statements, opinions and data contained in all publications are solely those of the individual author(s) and contributor(s) and not of MDPI and/or the editor(s). MDPI and/or the editor(s) disclaim responsibility for any injury to people or property resulting from any ideas, methods, instructions or products referred to in the content.